Experimental Flutter Suppression of a Long-Span Suspension Bridge Section

Kevin Gouder[+1], Xiaowei Zhao[+2], David Limebeer[+3] and J. Michael R. Graham[+4]
[+1, +4] Imperial College, London, United Kingdom
[+2]University of Warwick, Warwick, United Kingdom
[+3]University of Oxford, Oxford, United Kingdom

The suppression or delay of flutter in long-span suspension bridges is investigated experimentally. Since the torsional stiffness of a bridge deck decreases with increasing length, an active flap flutter suppression system could potentially enable the construction of longer spans without costly increases in deck width and depth. An active flap flutter suppression system could be deployed as a temporary measure during construction when the deck, not yet tied down at one or both ends, is particularly vulnerable to flutter instability. In the current experiment, a rigid sectional model of a long-span suspension bridge is mounted on a suspension system in a wind tunnel. Moving flaps attached to the bridge section's leading and trailing edges are controlled in real-time in response to the bridge section's heave and pitch motions. Other modes of bridge section motion, such as sway, were suppressed through the use of drag wires. Experimental assessment of the deck's aerodynamic derivatives and their similarity to those of a flat plate justified the aerodynamic force modeling using a theoretical model based on Theodorsen's theory; the flap control system is designed through an $\mathcal{H}_\infty$ optimisation. The control system design was constrained to low-order passive controllers that could be effectively replaced by reliable, passive (no external energy input) mechanical networks that drive the flaps through the bridge deck motion. The flutter-suppression effectiveness of various controllers with one or both actuated flaps, and different feedback quantities including one, or a combination of the bridge section's pitch angle and heave positions or velocities, was tested. Flutter velocity increases in excess of 20% were attained with very good robustness margins.

Keyword: flutter, wind-tunnel, long-span suspension bridge, robust control, flaps.

1. INTRODUCTION

Low structural damping[1)] and structural flexibility[2)] of cable-supported bridges makes them sensitive to wind-induced influences, where oscillatory or even divergent unstable modes may exist. Torsional flutter oscillation[3)] caused by a sign reversal in the aerodynamic derivative A_2^* related to torsional damping caused the Tacoma Narrows Bridge collapse when oscillations in the first asymmetric torsion mode grew over a period of about 45 minutes. Since this collapse, advances in deck design have prevented similar incidents but the flutter problem is still a formidable challenge owing to the need to construct longer spans with a resulting lower critical, flutter wind velocity. Deck stiffening, particularly in torsion, with the inevitable increases in cost and weight, is the traditional flutter delay effort. Adding a solid or porous spanwise beam along the deck centre-line, creating a gap between the carriageways, leading and trailing edges cross section modifications[4)], the addition of fairings and turning vanes around the leading and trailing deck edges[5)] have been proven beneficial in flutter delay. Such efforts have a limited capability in raising the flutter velocity and therefore research into active flow control has also been carried out. One active control method is based on controllable moving surfaces that respond to bridge deck motion. Flap control for aeroelastic load alleviation – flutter and buffet suppression – has already been successfully used in the aeronautics industry, where flap motions respond to suppress main wing motions [6)–11)]. In a long-span bridge deck setting, the concept has also been investigated for the suppression of flutter and buffet loads. A number of patents have been granted for systems

[+1]kevin.gouder04@imperial.ac.uk, [+2]xiaowei.zhao@warwick.ac.uk, [+3]david.limebeer@eng.ox.ac.uk, [+4]m.graham@imperial.ac.uk

that delay deck flutter using active flaps [12), 13)]. The scheme has also been the subject of research reported in the literature [14 – 22, 26, 27)]. The problem was theoretically investigated for cable-suspended bridges with flaps on both sides of the deck[16) – 20)].

Using unsteady thin aerofoil derivations by Theodorsen[23)], where the deck is treated as a 2D thin section on an elastic suspension, classical 2-DOF (heave and pitch) flutter is reasonably well modelled and good predictions of the flutter velocity can be obtained. When this analysis is applied to more realistic, thicker, bluffer cross-sections, the method could be supplemented with *measured* section aerodynamic derivatives within the reduced frequency range of interest. Strip theory is often utilised to extend the 2D section results to 3D deck modal response[24)]. The analysis of a wing-aileron-tab system[25)] was transformed and utilised for the aeroelastic control of a bridge deck with leading and trailing edge flaps, using an approximation for the leading edge flap[16)], and exactly[26)], where an increase in flutter velocity was shown to be feasible. A number of experimental implementations have also been reported. One variation of twin control surface implementation was tested[14)] where aerofoil flaps were suspended below a model deck, with the rather poor assumption[26)] that the deck and control surfaces in practical close proximity are aerodynamically independent of each other. An adoption of the same assumption, where a deck-mounted pendulum was the prime mover of the flap control system, led to good agreements with theoretical results, although only for small flap angles[27)]. Coupled deck-flap aerodynamics, albeit with an approximation for the leading-edge flap, were utilised in another experiment[16)], where measured control flap-induced aerodynamic damping performance was reported and compared to Theodorsen theory predictions.

This paper is an extension of an earlier study[21)] where flutter delay of a section of a long-span suspension bridge is experimentally and numerically investigated utilising Theodorsen theory (aerofoil with flap and tab transformed to represent a deck with leading and trailing edge flaps) and $\mathcal{H}_\infty$ optimisation. A 1:50 scale model of a representative bridge deck had controllable leading and trailing full-span flaps installed and was mounted on a suspension system with heave and pitch degrees of freedom. Although the flaps used in these experiments were along the whole span of the sectional model, it is envisaged that in a practical full-scale application, a number of part-span flaps would be installed straddling the bending and torsion flutter modes' antinodes. Wind tunnel tests were carried out in low-turbulence levels although the control system robustness was further assessed when grid-generated turbulence provided supplementary random perturbations[21)]. The tested flap controllers were limited to low order passive networks where passivity implies that springs, dampers and inerters could in principle be utilised to construct the control system. In [21], a number of controllers based on deck position feedback (heave, pitch, or a combination of the two to the leading edge, trailing edge or both flaps) were reported. The objective of this paper is to report about the performance of a number of other controller configurations, including one based on position feedback of the trailing edge flap hinge point and others based on the deck heave and/or pitch velocity, and compare their performance with the theoretical predictions.

Active control surface flutter delay could be one technology enabling the construction of longer deck spans. It also has the potential to be deployed as a temporary measure during bridge construction when both ends of the deck are still unconnected and the flutter velocity of either end is well below the design value for the completed superstructure. The rest of this paper is organised as follows. In Section 2 a summary of the theoretical model is presented, followed by a description and design of the control systems. A summary of the experimental setup is presented in Section 3 and results from a number of controller configurations presented in Section 4 and discussed shortly in Section 5.

2. THEORETICAL MODEL AND CONTROL SYSTEM DESIGN

In this section, the theoretical structural and aerodynamic models used in the analysis and design of the control systems are briefly described. Figure 1 shows the kinematic model of the bridge deck with flaps.

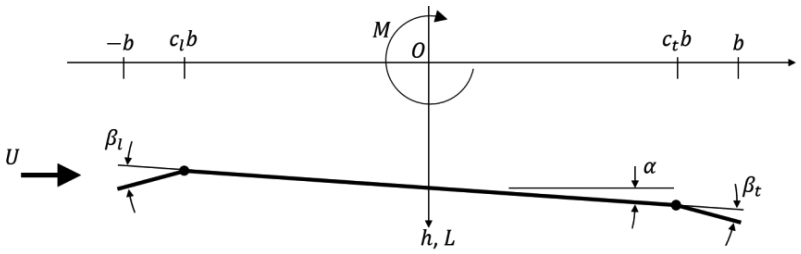

Deck chord (including flaps) = $2b$
Moment M (about centre chord) and pitch angle α positive clockwise
Lift L and heave h positive down
Leading-edge and trailing edge flap angles, β_l and β_t respectively, positive down

Figure 1: The kinematic model of the bridge deck with leading and trailing edge flaps.

Referring to Figure 1, the equations of motion for the two degrees of freedom, heave and pitch, of the deck model are:

$$M_h\left(\ddot{h} + 2\zeta_h\omega_h\dot{h} + \omega_h^2 h\right) = L \qquad \text{and} \qquad J_\alpha(\ddot{\alpha} + 2\zeta_\alpha\omega_\alpha\dot{\alpha} + \omega_\alpha^2\alpha) = M \tag{1}$$

where M_h is the deck mass and J_α is the deck moment of inertia about the mid-chord axis, both quantities defined per unit span of deck
L is Lift force and M is Moment about the mid-chord axis
ω_h, ζ_h and ω_α, ζ_α are the undamped natural frequency and damping ratio, respectively for heave (h) and pitch (α).

The aerodynamic model derived and used in this work was based on the wing-flap-tab system reported in (25). The Lift L and Moment M in equation (1) are a function of wind speed, heave, pitch and flap angles and their derivatives,

$$L = \rho b^3\omega^2\left(L_h\frac{h}{b} + L_\alpha\alpha + L_{\beta_t}\beta_t + L_{\beta_l}\beta_l\right) \text{ and } M = \rho b^4\omega^2\left(M_h\frac{h}{b} + M_\alpha\alpha + M_{\beta_t}\beta_t + M_{\beta_l}\beta_l\right). \tag{2}$$

The quantities L and M with subscripts within the brackets in equation (2) are aerodynamic derivatives, all a function of the Theodorsen function $C(k)$. Further details on the wing-flap-tab transformation into a deck with leading and trailing edge flaps can be found in reference [26].

Table 1: Details about controllers tested indicating which flaps were used, the corresponding feedback and the controller transfer function. The abbreviations LE and TE refer to the leading- and trailing-edge flaps; $\alpha, \dot{\alpha}, h, \dot{h}$ refer to pitch position, pitch velocity, heave position and heave velocity feedbacks respectively.

Type	#	Flap (s) : Feedback	Transfer function
Position Feedback	1	TE : $h + 0.407\alpha$	$\frac{-59.9059s}{s^2 + 14.8262s + 147.9288}$
Mechanical Controller (velocity feedbacks)	2	LE : $\dot{h} - 0.407\dot{\alpha}$	$\frac{305.4957\text{s}}{107.9075\text{s}\hat{}2 + 1072.55\text{s} + 24629.33}$
	3	TE : $\dot{h} + 0.407\dot{\alpha}$	$\frac{150.286\text{s}}{65.475\text{s}\hat{}2 + 1238.746\text{s} + 29060.9333}$
	4	LE : $\dot{h} - 0.407\dot{\alpha}$ TE : $\dot{h} + 0.407\dot{\alpha}$	$\frac{392.455\text{s}}{66.7287\text{s}^2 + 2137.2609\text{s} + 42636.1042}$ to both flaps.

Based on the root locus analysis, it was established that the theoretical critical flutter speed was 20 m/s (see Figure 6 of reference [21]). The control aim was to improve the critical flutter speed to 24 m/s, therefore to a wind speed lower than the predicted divergence speed. $\mathcal{H}_\infty$ theory was used to design the flutter controller; see Figure 5 of reference [21] for the control system configuration. The details about the control design can be found in reference [21]. The designed controllers are summarised in Table 1 including which flap is active, what feedback its controller receives and the controller's transfer function. Controller 1 receives deck position feedback while controllers 2 to 4 receive velocity feedback. The constant 0.407 in the feedback expressions refers to the position, in metres, of the hinge point relative to the centre-chord origin. All controllers are low order passive networks as described earlier, although controllers 2 to 4 are explicitly designed using passive mechanical components. The root locus of the closed-loop systems with these controllers are shown in Figure 2, showing that the heave, pitch, and torsional divergence modes are all well damped up to 24 m/s, i.e. 20% improvement in theory. It was expected that similar flutter alleviation improvements were possible in the wind tunnel experiments using these controllers.

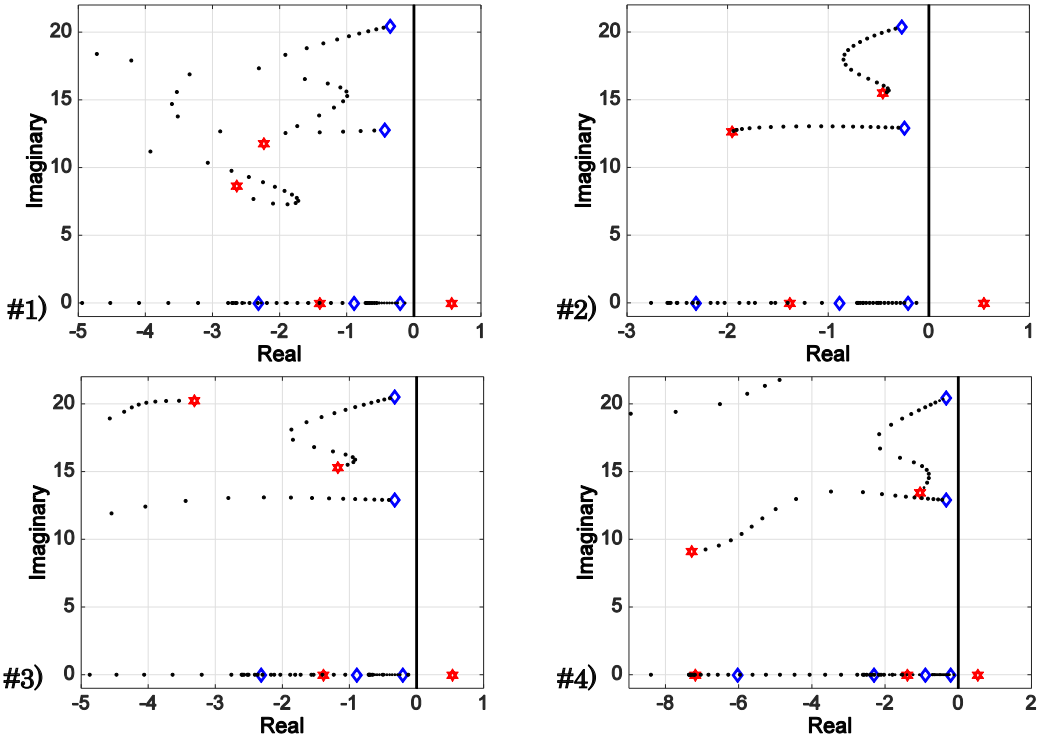

Figure 2: Root loci of the controllers shown in Table 1. The wind speed is swept from 5 to 25 m/s, with the low-speed end of the root loci marked with blue diamonds and the high-speed ends marked with red hexagons.

3. EXPERIMENTAL SETUP

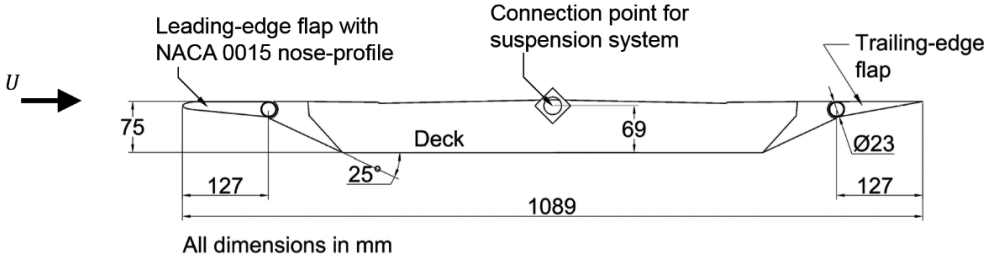

Figure 3: A schematic of the cross-section of the bridge deck model. The model is a 1:50 scale reconstruction of a prototype previously tested at BMT Fluid Mechanics.

The bridge deck utilised in these experiments is a rigid structure made from carbon-fibre-reinforced composite material with chord 0.82 m, span of 2.74 m and a depth of 0.075 m. The original deck's leading- and trailing-edges were faired using low-density styrofoam so that the cross-section was made identical to a proposed long-span crossing design previously tested at BMT Fluid Mechanics. Flap-type control surfaces were installed along the whole span at the deck leading- and trailing-edges. Each flap had a chord of 12% of the total deck chord, which, including fairings and both flaps, had a total chord of 1.09 m. The flaps initially had a triangular cross section and although flow separation observed occurring at the sharp leading edge of the upstream flap was potentially causing additional buffet loading, this did not appear to be reducing control performance. However, for all experiments reported here, the leading-edge of the upstream flap was slightly rounded following a NACA0015 profile, (3 mm nose curvature), in order to inhibit separation there and improve the accuracy of linear theory (where the deck and control surfaces are treated as aerodynamically thin) in predicting deck response. The trailing edge flap was however not modified since a rounded trailing edge reduces control surface effectiveness. But where extreme winds normal to the deck are possible from either side, rounding of both flaps could be required and further work is needed. The natural frequency of the two flap control surfaces around their hinge-lines, $\omega_{\beta l}$ and $\omega_{\beta t}$, were substantially high so that at any velocity tested here, the flaps did not experience any form of excitation that could have caused early deck flutter through a deck-flap interaction. Two Nanotec ST8918S4508 NEMA34 3 Nm stepper motors were utilised, each driving one flap control surface through a 1:5 reduction gearbox located at one end of an aluminium shaft running along the span. A Nanotec SMCI47-S stepper motor positioning controller controlled each motor in analogue positioning mode where an analogue voltage input was proportional to motor shaft position. A Nanotec WEDS5541-B shaft encoder (4000 counts per revolution) was utilised for shaft positional feedback. An internal, hardware, PID controller monitored shaft demand and actual positions, governed corrections and ensured shaft positional fidelity.

An H-assembly of springs (each of stiffness 1160 N/m) suspension system, either side of the tunnel test section allowed deck pitch and heave degrees of freedom. The heave frequency depended on the deck mass and the combined stiffness of the two spring H-assemblies (8 springs in total); the pitch frequency, on the other hand, could be adjusted by varying the horizontal separation between two arms of the springs H-assembly[21]. The deck's roll degree of freedom was unconstrained but this mode was never excited, owing to the aerodynamic forces being predominantly 2-dimensional given that the deck spanned the tunnel width. The bottom of each arm of the H-assembly was connected to a load-cell and so through the known spring stiffnesses, the heave and pitch positions of the deck were inferred. Further details about the setup can be found in reference [21]. The deck was balanced such that it had no static moment making the term a equal to zero in equations XVIII-XX[23]. The deck still attained a small mean incidence in tests, mainly due to the position of the aerodynamic centre close to the deck's quarter chord position and also due to the deck's cambered cross-section. Spanwise and streamwise sway modes were constrained through drag wires connected to the deck through small leaf-springs in order to avoid the introduction of damping. The measured structural heave and pitch damping ratios were $\zeta_h = 0.0057$ and $\zeta_\alpha = 0.0033$ respectively, or $\delta_h = 0.036$ and $\delta_\alpha = 0.021$ in log-dec representation.

BMT Fluid Mechanics provided full-scale prototype properties, specifically a deck bending frequency $f_B \approx 0.29$ Hz and a torsional frequency $f_T \approx 0.45$ Hz giving a frequency ratio $f_T/f_B = 1.51$. The full-scale mass ratio $M_h/\rho A_x \approx 190$, where M_h is the deck mass per unit length and A_x is an area defined as the deck chord $2b \times$ deck depth. Both the frequency ratio and the mass ratio of the model were matched to those of the full-scale prototype. Since the model utilised here is a stiff section model where the mode frequencies are defined by the springs in the external suspension system, the Froude number was not matched to that of the full-scale prototype. This dimensionless group only becomes important when part of the structural stiffness is provided by gravitational forces, for example when full 3D model testing of a suspension bridge is performed[28]. The Reynolds number based on deck chord was just above 1×10^6.

Table 2: Parameters of the model bridge deck used in these experiments.

Parameter	Value	Parameter	Value
b (half-chord incl. flap)	0.545 m	M_h	18.9 kg
ρ	1.23 kg/m^3	J_α	1.8 kg m^2
		ω_h	13.45 rad/s
		ω_α	20.74 rad/s

Using data from Table 2, the flutter velocity was predicted at 19.4 m/s (Selberg's formula) and at 20.1m/s using codes based on Theodorsen thin-aerofoil theory and a vortex-panel method. The theoretical values were corrected using a correction factor[2)] for predicted thin-aerofoil theory flutter velocity applied to non-thin bodies, to between 16 and 18 m/s. Experimentally, the flutter velocity was obtained through a number of experiments where the rate of decay or growth of oscillations was noted and the velocity at $\zeta = 0$ evaluated. A value of 17.5 m/s was obtained and will be adopted henceforth as the critical, flutter velocity. The divergence speed was estimated to be around 28.5 m/s, around 62% higher than the measured flutter speed and therefore beyond the percentage increases in flutter speed attained through the current flap control system. Experiments were run at the tunnel no. 5 at BMT Fluid Mechanics with a test-section width 2.75 m and height of 2.7 m, and in the Honda tunnel at Imperial College with a test section of 3 m by 1.5 metres; the deck exactly spanned the tunnel in the former case, while false walls were utilised in the Honda tunnel.

4. RESULTS

Results from the four tested controllers of Table 1 are presented in this section. The left-hand subfigure in each of Figures 4 to 7 shows typical tests where at a velocity 15% above the flutter velocity, the control was repeatedly toggled open (indicated by the red dashed vertical line) allowing oscillations to grow naturally. The control was subsequently toggled closed (indicated by the green dashed vertical line) allowing the control surfaces to impart the necessary control to dampen the oscillations. The damping performance was evaluated by computing the damping ratio of the deck's assumed second order response as described in reference [21]. Each right-hand figure shows the evolution of the damping ratio, for both the heave and pitch modes, with freestream velocity for various gains. The reason behind the repeat of experiments for various gains is explained in the next section.

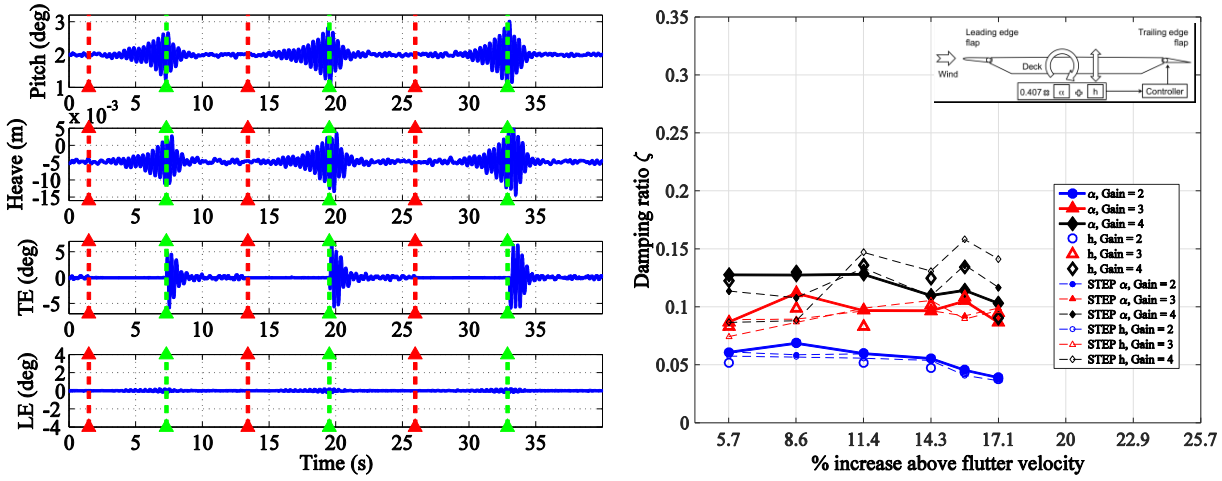

Figure 4: Controller #1: *Left*: Time-traces of the pitch and heave positions of the deck, and the corresponding trailing- and leading-edge flaps angles. The leading edge flap is held rigid while the trailing edge flap has a combination of deck heave and pitch position feedback, as shown in the inset sub-figure on the Right. The gain of the trailing-edge flap actuator is 3, and the wind velocity is 15% higher than flutter. *Right*: The evolution of the closed-loop damping ratio ζ as a function of %velocity increase above the flutter velocity. The gain (multiplier of theoretical flap angle demand) is varied from 2 to 3 to 4 at each velocity.

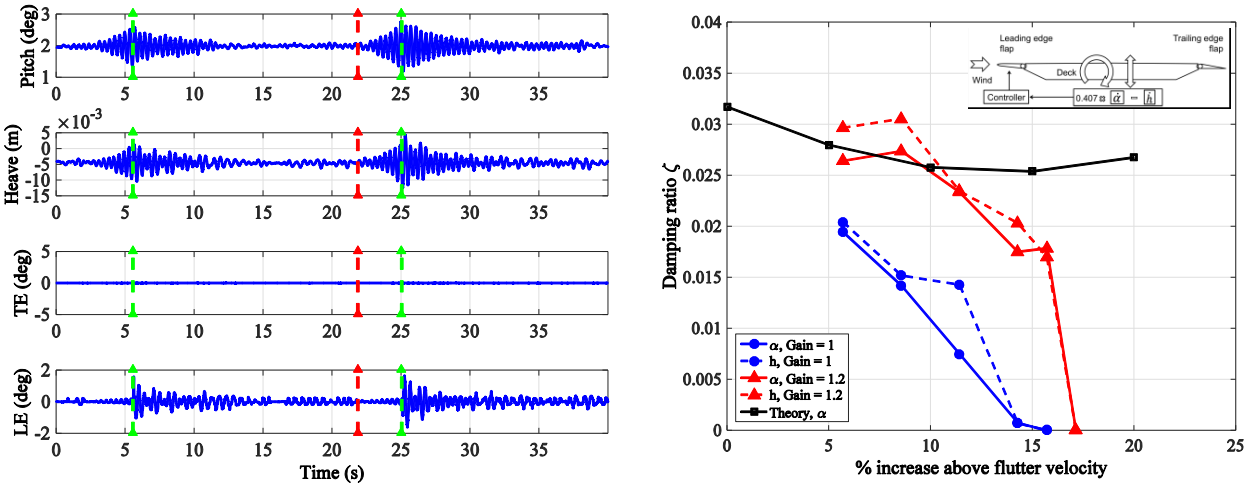

Figure 5: Controller #2: *Left*: Time-traces of the pitch and heave positions of the deck, and the corresponding trailing- and leading-edge flaps angles. The trailing edge flap is held rigid while the leading edge flap has a combination of deck heave and pitch **velocity** feedback. The gain of the leading-edge flap actuator is 1.2, and the wind velocity is 15% higher than flutter. *Right*: The evolution of the closed-loop damping ratio ζ as a function of %velocity increase above the flutter velocity. The gain is varied to 1 and 1.2 at each velocity.

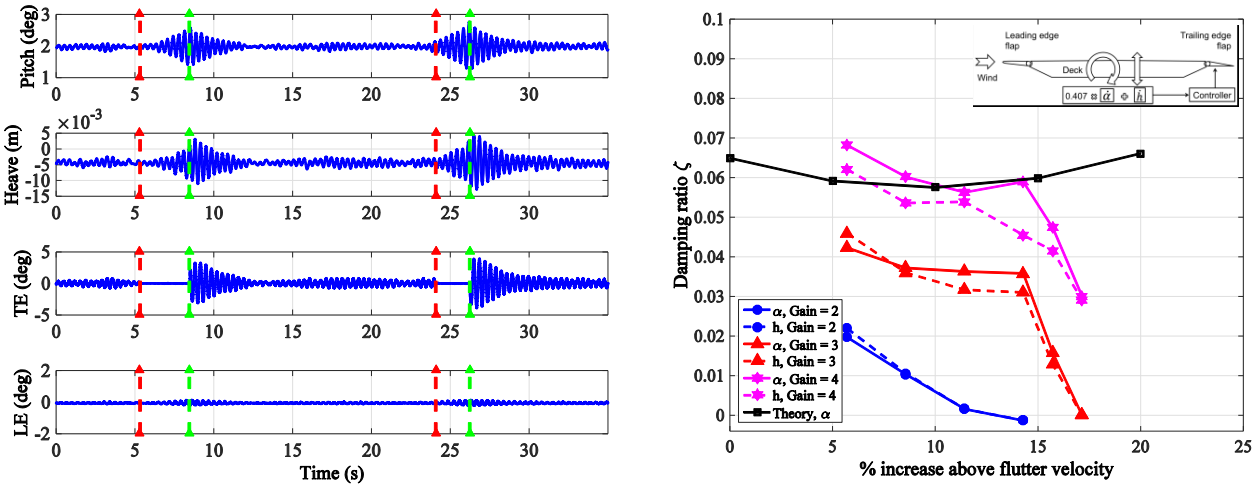

Figure 6: Controller #3: *Left*: Time-traces of the pitch and heave positions of the deck, and the corresponding trailing- and leading-edge flaps angles. The leading edge flap is held rigid while the trailing edge flap has a combination of deck heave and pitch **velocity** feedback. The gain of the trailing-edge flap actuator is 3, and the wind velocity is 15% higher than flutter. *Right*: The evolution of the closed-loop damping ratio ζ as a function of %velocity increase above the flutter velocity. The gain is varied to 2, 3 and 4 at each velocity.

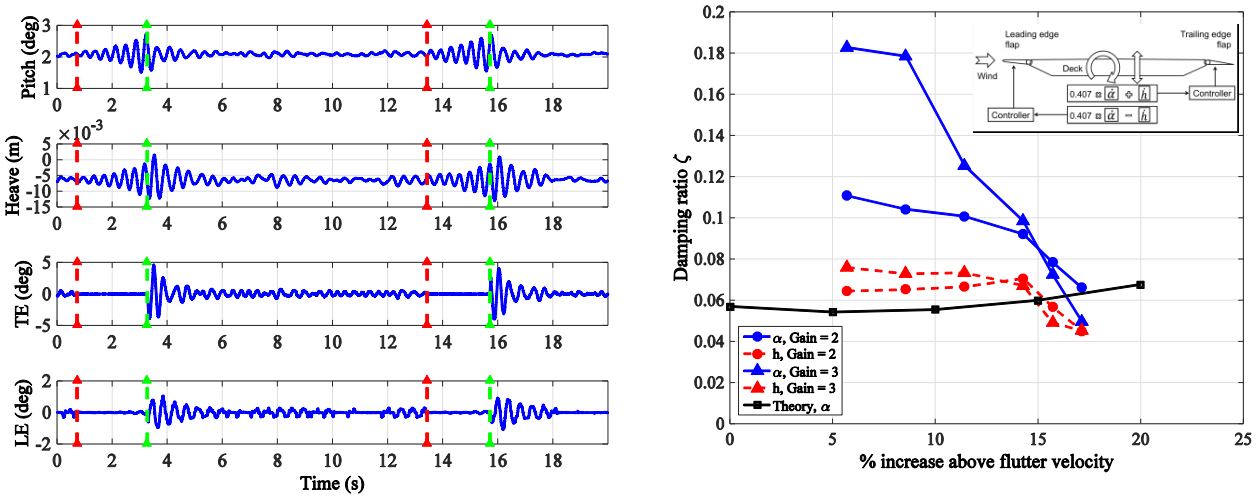

Figure 7: Controller #4: *Left*: Time-traces of the pitch and heave positions of the deck, and the corresponding trailing- and leading-edge flaps angles. The leading edge flap and trailing edge flaps have a combination of deck heave and pitch **velocity** feedback. The gain of the trailing-edge flap actuator is 3, and the wind velocity is 15% higher than flutter. *Right*: The evolution of the closed-loop damping ratio ζ as a function of %velocity increase above the flutter velocity. The gain of the leading edge flap was equal to 1 and that of the trailing edge flap is varied between 2 and 3 at each velocity.

5. DISCUSSION

The gain of the leading edge flap controller was in most cases set to 1 while that for the trailing edge flap controller was varied between 2 and 4. This increase in gain above the theoretical value of 1 was followed to compensate for the effects of the trailing edge flap operating in the separated wake of the deck. This is observed in Figure 8 showing a pressure distribution around the deck as well as from flow visualisation. The reduced effectiveness of the trailing edge flap was also observed through measurements of $\mathrm{d}C_L/\mathrm{d}\beta_t$ and $\mathrm{d}C_M/\mathrm{d}\beta_t$ as reported in Figures 22 and 23 of reference [21].

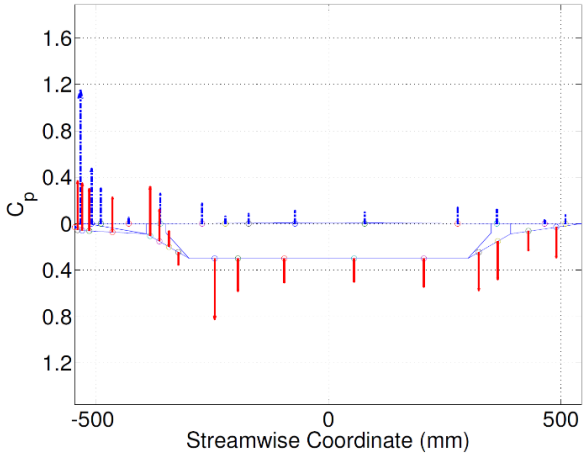

Figure 8: Pressure distribution around the deck at a velocity just below the onset of flutter (flow is from left to right). It was confirmed the trailing edge flap is operating in the deck wake and at reduced effectiveness.

Fair agreement was obtained between the theoretical damping ratios (extracted from the Root-Locus figures) and the values obtained experimentally. Good agreement was attained for Controllers 2 and 3, albeit at experimentally raised gain. For controller 4, for both tested gains, the experimental results indicate a better

performance than that predicted. Differences (though not very significant) in aerodynamic derivatives between the theoretical and measured ones were deemed responsible for the discrepancy between the theoretical and experimental values of the flutter velocity and controller performances[21]. In this work, the controllers were designed using the theoretical aerodynamic derivatives and no attempt was made to introduce any corrections for the discrepancies indicated by measured aerodynamic derivatives. This was done in order to justify using the theoretical model for decks which are quasi-streamline like some trapezoidal section modern decks.

6. CONCLUSIONS

In this work, an extension of the work reported in reference [21], the performance in delay of the onset of flutter was reported for a number of leading-edge and trailing-edge flap controllers and feedbacks. Pitch and heave position and velocity feedbacks were investigated in conjunction with the use of the leading-edge, trailing-edge or both flaps. The controllers were based around thin aerofoil theory even though aerodynamic derivative measurements showed some discrepancies with their theoretical, utilised, counterparts. This approach was to justify and demonstrate the retention of controller effectiveness at least for decks which are streamlined or quasi-streamlined. The controllers reported here were found to delay the flutter velocity by an estimated (extrapolated) 20% (closely matching the theoretical predictions) and were based around the use of passive mechanical elements, increasing the chances of survivability of the system in extreme conditions.

ACKNOWLEDGMENTS

The authors would like to thank the Engineering and Physical Sciences Research Council (UK) grant number EP/H029982/1 and by BMT Fluid Mechanics Ltd who supported this work. The additional wind tunnel time granted by BMT and the support and advice given by their staff S. Cammelli and A. Elliot is gratefully acknowledged. They would also like to thank Prof. T. Wyatt for his many insights and invaluable advice.

REFERENCES

1) Schlaich, M., Brownlie, K. , Conzett, J., Sobrino, J., Strasky, J. and Takenouchi, K., Guidelines for the design of footbridges: Guide to good practice, Int. Fed. Struct. Concrete, Lausanne, Switzerland, Tech. Rep., 2005.
2) Dyrbye, C. and Hansen, S. O., Wind Loads on Structures, 1st ed. Chichester, U.K.: Wiley, 1999.
3) Billah, K. Y. and Scanlan, R. H., Resonance, Tacoma Narrows bridge failure, and undergraduate physics textbooks, Amer. J. Phys., vol. 59, no. 2, pp. 118–124, 1991.
4) Larsen, A., Savage, M., Lafreniére, A., Hui, M. C. H., and Larsen, S. V., Investigation of vortex response of a twin box bridge section at high and low Reynolds numbers, J. Wind Eng. Ind. Aerodyn., vol. 96, nos. 6–7, pp. 934–944, 2008.
5) Larsen, A., Esdahl, S., Andersen, J. E., and Vejrum, T., Storebælt suspension bridge—Vortex shedding excitation and mitigation by guide vanes, J. Wind Eng. Ind. Aerodyn., vol. 88, nos. 2–3, pp. 283–296, 2000.
6) Triplett, W. E., 1972. A feasibility study of active wing/store flutter control. J. Aircraft 9 (6), 438–444.
7) Triplett, W. E., Kappus, H. P. F., Landy, R. J., 1973. Active flutter control - an adaptable application to wing/store flutter. J. Aircraft 10 (11), 669–678.
8) Roger, K. L., Hodges, G. E., Felt, L., 1975. Active flutter suppression – a flight test demonstration. J. Aircraft 12 (6), 551–556.
9) Karpel, M., 1982. Design for active flutter suppression and gust alleviation using state-space aeroelastic modeling. Journal of Aircraft 19 (3), 221–227.
10) Borglund, D., Kuttenkeuler, J., 2002. Active wing flutter suppression using a trailing edge flap. Journal of Fluids and Structures 16 (3), 271 – 294.
11) Burnett, E., Atkinson, C., Sibbitt, B., Holm-Hansen, B., Nicolai, L., 2010. Ndof simulation model for flight control development with flight test correlation. In: AIAA Modeling and Simulation Technologies

Conference, Toronto, Canada, AIAA paper 2010-7780.
12) Ostenfeld, K. H., A system and a method of counteracting wind induced oscillations in a bridge girder, European Patent 0 627 031 B1, Jun. 12, 1996.
13) Corney, J. M., Bridge stabilization, WO Patent 1997 045 593, Dec. 4, 1997. [Online]. Available: http://www.google.com.ar/patents/ WO1997045593A1?cl=en
14) Kobayashi, H. and Nagaoka, H., Active control of flutter of a suspension bridge, J. Wind Eng. Ind. Aerodyn., vol. 41, nos. 1–3, pp. 143–151, 1992.
15) Ostenfeld, K. H. and Larsen, A., Bridge engineering and aerodynamics, in Proc. 1st Int. Symp. Aerodyn. Large Bridges, 1992, pp. 3–22.
16) Hansen, H. I. and Thoft-Christensen, P., Active flap control of long suspension bridges, J. Struct. Control, vol. 8, no. 1, pp. 33–82, 2001.
17) Wilde, K. and Fujino, Y., Aerodynamic control of bridge deck flutter by active surfaces, J. Eng. Mech., vol. 124, no. 7, pp. 718–727, 1998.
18) Omenzetter, P., Wilde, K., and Fujino, Y., Suppression of wind-induced instabilities of a long span bridge by a passive deck–flaps control system: Part I: Formulation, J. Wind Eng. Ind. Aerodyn., vol. 87, no. 1, pp. 61–79, 2000.
19) Omenzetter, P., Wilde, K., and Fujino, Y., Suppression of wind-induced instabilities of a long span bridge by a passive deck-flaps control system: Part II: Numerical simulations, J. Wind Eng. Ind. Aerodyn., vol. 87, no. 1, pp. 81–91, 2000.
20) Nissen, H. D., Sørensen, P. H. and Jannerup, O., Active aerodynamic stabilisation of long suspension bridges, J. Wind Eng. Ind. Aerodyn., vol. 92, no. 10, pp. 829–847, 2004.
21) Gouder, K., Zhao, X., Limebeer, D., Graham, J., 2015. Experimental aerodynamic control of a section of long-span suspension bridge using leading and trailing-edge control surfaces. IEEE Trans Control System Technology. In press. DOI:10.1109/TCST.2015.2501346
22) Zhao, X., Gouder, K., Graham, J., Limebeer, D., 2015. Buffet Loading, Dynamic Response and Aerodynamic Control of a Suspension Bridge in a Turbulent Wind, Journal of Fluids and Structures. In press.
23) Theodorsen, T., General theory of aerodynamic instability and the mechanism of flutter, NASA Langley Res. Center, Hampton, VA, USA, Tech. Rep. NACA-TR-496, 1934.
24) Massaro, M. and Graham, J. M. R., The effect of three-dimensionality on the aerodynamic admittance of thin sections in free stream turbulence, J. Fluids Struct., vol. 57, pp. 81–90, Aug. 2015.
25) Theodorsen, T. and Garrick, I. E., Nonstationary flow about a wing-aileron-tab combination including aerodynamic balance, NASA Langley Res. Center, Hampton, VA, USA, Tech. Rep. NACA-TR-736, 1942.
26) Graham, J. M. R., Limebeer, D. J. N. and Zhao, X., Aeroelastic control of long-span suspension bridges, ASME J. Appl. Mech., vol. 78, no. 4, pp. 041018-1–041018-12, 2011.
27) Wilde, K. Fujino, Y. and Kawakami, T., Analytical and experimental study on passive aerodynamic control of flutter of a bridge deck, J. Wind Eng. Ind. Aerodyn., vol. 80, nos. 1–2, pp. 105–119, 1999.
28) Holmes, J. D., Wind Loading of Structures. Boca Raton, FL, USA: CRC Press, 2015.